ACS OMEGA

http://pubs.acs.org/journal/acsodf

Article

Fabrication of Polysulfobetaine Gradient Coating via Oxidation Polymerization of Pyrogallol To Modulate Biointerfaces

Piyush Deval, Chia-Hsuan Lin, and Wei-Bor Tsai*

Cite This: *ACS Omega* 2022, 7, 7125−7133

Read Online

ACCESS | Metrics & More | Article Recommendations | Supporting Information

ABSTRACT: A surface with a gradient physical or chemical feature, such as roughness, hardness, wettability, and chemistry, serves as a powerful platform for high-throughput investigation of cell responses to a biointerface. In this work, we developed a continuous antifouling gradient surface using pyrogallol (PG) chemistry. A copolymer of a zwitterionic monomer, sulfobetaine methacrylate, and an amino monomer, aminoethyl methacrylate, were synthesized (pSBAE) and deposited on glass slides via the deposition of self-polymerized PG. A gradient of pSBAE was fabricated on glass slides in 7 min in the presence of an oxidant, ammonium persulfate, by withdrawing the reaction solution. The modified glass slide showed a wettability gradient, determined by measuring the water contact angle. Cell adhesion and protein adsorption were well correlated with surface wettability. We expect that this simple and faster method for the fabrication of a continuous chemical gradient is applicable for high-throughput screening of surface properties to modulate biointerfaces.

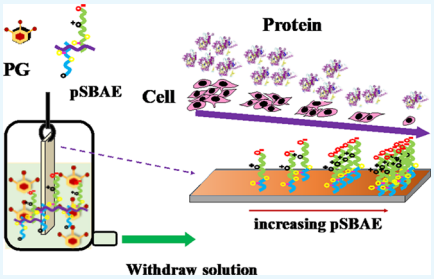

1. INTRODUCTION

Adhesion, spread, growth, and differentiation of cells on a surface are important aspects for cell responses to biomaterials. A surface with a "gradient" feature, such as roughness, hardness, wettability, surface energy, or chemistry, acts as a powerful tool for the systematic investigation of cell behavior in response to physiochemical parameters of various biomaterials.[1,2] Surfaces with a gradient of hydrophilicity−hydrophobicity, softness-hardness, biomolecule/polymer concentration, roughness, or pore size have served as a high-throughput platform for the investigation of cell interactions with surfaces of biomedical devices.[3−8] Numerous techniques have been employed to fabricate gradient surfaces such as gradual immersion/retraction,[9] microstamping,[10] microfluidic lithography,[11] electrochemical,[6,12] plasma treatment,[13,14] corona irradiation,[15,16] UV photolithography,[17,18] chemical degradation,[19] diffusion,[20] and polymer curing.[8] Among these methods, gradual immersion/retraction of samples into/from a solution of monomers, solvents, or etchants, thus creating a gradient based on immersion/retraction rate, is a simple and common method to fabricate a continuous gradient.

A gradient of cell adhesion could be achieved on a surface with a concentration gradient of an antifouling polymer. Antifouling polymers, including polysaccharides, poly(ethylene glycol) (PEG), poly(vinyl alcohol), poly(*N*-vinylpyrrolidone), and poly(zwitterions), are highly hydrophilic and adsorb a great amount of water to form a barrier to reduce nonspecific cell adhesion and protein adsorption. Surface immobilization of antifouling polymers could resist or reduce cell adhesion. In recent years, zwitterionic polymers such as poly(2-methacryloyloxyethyl phosphorylcholine), poly(sulfobetaine methacrylate), and poly(carboxybetaine methacrylate) have been increasingly used because of their excellent low-fouling properties.[21−27] Zwitterionic monomers contain one cationic and one anionic group, which leads to strongly bound water molecules.[23,28,29] A previous study showed that grafting poly(sulfobetaine) to surfaces reduced nonspecific protein adsorption to less than 0.3 ng/cm^2 from single protein solutions.[30] Zwitterionic polymers have been applied in various biomedical applications because of their excellent antifouling ability.[31−41]

Antifouling polymers could be conjugated on a substrate in a gradient manner, thus resulting in a cell adhesion gradient. For example, PEG attached to positively charged polylysine was adsorbed on a negatively charged titanium dioxide surface through electrostatic interactions in a time-dependent manner; thus, a PEG coverage gradient was created on titanium dioxide surfaces to modulate cell adhesion and spreading.[42] A poly(methacryloyloxyalkyl-phosphorylcholine) gradient surface was created using a corona discharge treatment to generate a cell gradient.[15] Ren and coworkers fabricated two-component gradient of a zwitterionic sulfobetaine polymer and a KHIFSDDSSE peptide using the controlled reaction method by solution injection, which was used to study cell adhesion and the migration of Schwann cells and fibroblast cells.[43]

Received: December 1, 2021
Accepted: February 1, 2022
Published: February 16, 2022

The objective of this study was to develop a simple and universal method to create a gradient surface of poly(sulfobetaine) for gradient cell adhesion/protein adsorption. Recently, we developed a simple one-step method for the fabrication of low-fouling coatings of zwitterionic polymers via pyrogallol (PG) deposition.[44] PG, a polyphenolic molecule, could spontaneously undergo polymerization into a robust coating on a wide variety of substrates under mild alkaline conditions.[45] Similar to coatings based on dopamine[46] and aminomalononitrile,[47] PG coating has strong and universal interfacial adhesiveness to substrates and chemical reactivity toward nucleophiles, such as amines and thiols.[48] Previously, we applied the mechanism to the immobilization of antifouling polymers, such as poly(ethylene glycol) and poly(sulfobetaine) on surfaces of several biomaterials using their copolymers with primary amine monomers and then immobilized the copolymers to several substrates via dopamine, aminomalononitrile, and polypyrogallol coatings to effectively inhibit cell adhesion.[44,49−51] In this study, we would like to extend the coating technology to the creation of gradient surfaces.

In this study, a copolymer (pSBAE) of sulfobetaine methacrylate (SBMA) and 2-aminoethyl methacrylate (AEMA) was synthesized and then deposited onto glass slides via PG deposition. The AEMA moiety provides anchorage to polypyrogallol via Michael addition.[52] PG forms polypyrogallol via oxidation,[53] so oxidizing agents were added to expedite the process. The pSBAE gradient was created on glass slides using a solution draining method. The coating was expedited via the addition of oxidizing agents. The formation of a pSBAE gradient was verified using the water contact angle (WCA) measurement, X-ray photoelectron spectroscopy (XPS), and atomic force microscopy (AFM). The adhesion of L929 and MG-63 cells was investigated as well as the adsorption of bovine serum albumin (BSA) on the gradient substrates. Finally, cell adhesion and protein adsorption were correlated with the surface gradient.

2. RESULTS AND DISCUSSION

2.1. Synthesis and Characterization of pSBAE. The pSBAE yield was ∼53%. The water solubility of the copolymer was poor but well soluble in 0.1 M phosphate buffer (pH 7.4). It is probably due to inter-zwitterion interactions between the sulfonate and quaternary ammonium groups of SBMA, which limits its solubility in water.[54] The interactions could be overcome in the presence of salts. The molecular weight of the copolymer was determined as ∼130 kDa using gel permeation chromatography. The monomer composition of the copolymer was determined using ^{1}H NMR (Figure S1 in the Supplementary Materials). Peaks at 3.75 and 4.2 ppm are associated with SBMA and AEMA, respectively.[49] The ratio of the integral areas of the two peaks was used as the molar ratio of SBMA to AEMA in pSBAE. The molar ratio of AEMA in pSBAE was estimated to be 9%, close to 10% AEMA in the monomer mixture.

2.2. Formation of Poly(PG) in the Presence of Oxidizing Agents. PG polymerization under alkaline conditions with oxidizing agents is a time-consuming process, usually requiring several hours. It is not a reasonable duration for the fabrication of gradient surfaces. Various oxidizing agents, such as ammonium persulfate [$(NH_4)_2S_2O_8$], methanol, sodium periodate ($NaIO_4$), and copper sulfate ($CuSO_4$), have been shown to facilitate the polymerization of dopamine and polyphenols.[55−58] Therefore, we used oxidizing agents to accelerate the PG coating.

The oxidative polymerization of PG turns the originally transparent solution dark brown, so the degree of PG oxidization could be visually evaluated based on the color of a PG solution. In this study, several oxidizing agents were tested: ammonium persulfate (APS), sodium persulfate, sodium periodate, potassium iodate, copper sulfate, potassium chlorate, and 20% methanol. Potassium iodate, sodium periodate, and copper sulfate turned the PG solution dark brown immediately after the addition of these oxidizing agents (Figures S2−S4), showing a very strong oxidizing property even at low concentrations. Fast reactions make it difficult to control the coating process. On the other hand, potassium chlorate and 20% methanol did not significantly speed up PG polymerization (Figures S5 and S6). They turned the PG solution light brown after 3 h. Sodium persulfate had a moderate oxidizing capacity but turned the PG solution turbid (Figure S7). We found that APS seems to meet our requirements, turning the PG solution dark brown in a couple of minutes (Figure 1). The speed of PG oxidation is dependent on the PG/APS molar ratios. Equal-molar PG/APS formed brown precipitates very quickly to be suitable for surface coating. The PG/APS solution at a molar ratio of 2 became dark brown in ∼3 min without apparent precipitates. The transition time increased further with increasing PG/APS

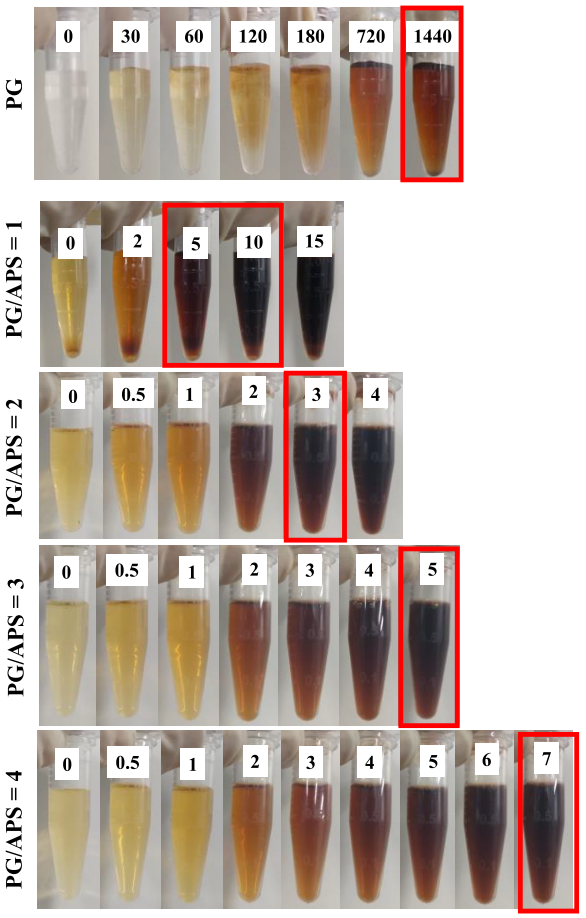

Figure 1. Oxidative polymerization of PG (8 mg/mL) in the presence of APS for different PG/APS molar ratios (1, 2, 3, and 4) at pH 7.4. The numbers indicate the incubation times (minutes).

https://doi.org/10.1021/acsomega.1c06798
ACS Omega 2022, 7, 7125−7133

ratios, indicating that PG oxidation could be controlled by varying APS concentrations. Thus, APS was chosen as the oxidizing agent for PG/pSBAE coatings.

Next, we tested the deposition of PG/pSBAE in the presence of APS to inhibit cell adhesion. In this experiment, the concentrations of PG and pSBAE were fixed at 8 and 40 mg/mL, respectively, with various amounts of APS. From PG/APS molar ratios of 0.5~4, cell adhesion to PG/pSBAE was significantly decreased compared to PG (Figure 2). The lowest cell adhesion appeared on the substrate with a PG/APS molar ratio of 3 (weight ratio ~ 1.66). Thus, the ratio was chosen to create a gradient pSBAE substrate.

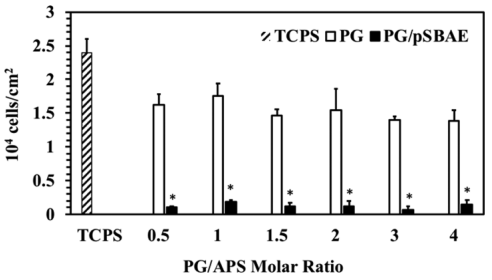

Figure 2. L929 cell adhesion on the pristine TCPS, PG, or PG/pSBAE-modified TCPS. The concentrations of PG and pSBAE were 8 and 40 mg/mL, respectively, with different PG/APS molar ratios. The coating time was 7 min. Value = mean ± standard deviation, $n = 3$. *, $p < 0.001$ vs PG.

2.3. Fabrication and Characterization of the pSBAE Gradient. Our previous study showed that one-step coating of PG/pSBAE could effectively inhibit cell adhesion.[44] Therefore, we tried creating a gradient of PG/pSBAE by the one-step process in the presence of APS, but could not achieve a constant gradient for cell adhesion. Therefore, two modifications of the process were used to improve gradient fabrication. First, the glass substrates were premodified in PG solution for 2 min to improve the coating efficiency of the subsequent PG/pSBAE coating. Second, in the literature, gradient substrates were frequently created via the immersion and removal method. Thus, we first tried immersing a glass slide into the PG/pSBAE/APS solution and gradually pulled the glass slide up. However, no constant gradient could be obtained. Thus, we used a different approach in which PG/pSBAE/APS solution was gradually drained from the bottom of the sample tube. We found that the formation of the gradient was more consistent and stable, so the PG/pSBAE gradient was fabricated using the draining method (see Section 4.3). Therefore, the glass slide was divided into three areas: pristine glass, PG, and the gradient (Figure 10).

We would like to investigate the surface gradient formation from 0 cm at the border of the PG area and the gradient area to the end of the gradient area. Therefore, the surface properties of the modified glass slides were characterized from the PG/gradient interface (i.e., 0 cm) to the positions that were 0.4, 0.8, 1.2, and 1.6 cm away from the border (Figure 10). However, the 0 cm line, which was supposed to be PG without pSBAE, was not clear-cut because of the fluctuation of the liquid interface, so its surface characterization was performed on the PG area. Gradient formation was first investigated according to the WCAs along the glass slides. The WCA on the pristine glass was 65.4°, while the PG coating decreased the WCA to 54.5° (Figure 3), indicating that the PG

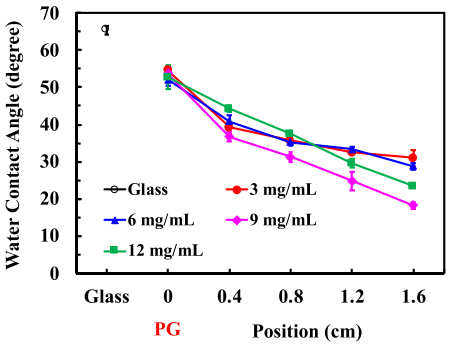

Figure 3. WCA measurement at different locations over the gradient glass slide: glass, 0 (PG), 0.4, 0.8, 1.2, and 1.6 cm. The gradient was created on a glass slide from a solution of PG (6 mg/mL)/pSBAE (40 mg/mL) with different APS concentrations from 3 to 12 mg/mL.

coating improves the wettability of the glass. After gradient deposition of PG/pSBAE, the WCA decreased further, varying with APS concentrations. In the presence of 3 mg APS/mL, the WCA decreased from 54.5° to 39.2°, 35.7°, 32.4°, and 31.1° at locations of 0.4, 0.8, 1.2, and 1.6 cm apart from the PG area, respectively. The steepest hydrophilicity gradient appeared in the presence of 9 mg APS/mL, resulting in the smallest WCA of 18.21° at 1.6 cm. Therefore, 9 mg APS/mL was used for the subsequent gradient coating to resist cell adhesion and protein adsorption.

XPS was used to determine the elemental composition at different locations along the gradient slides. The Si signal comes from the glass substrate and is expected to decrease with increasing coating. Sulfur, which comes from the SB moiety of pSBAE, is an indicative element for the pSBAE coating. It is expected that the sulfur content increases with increasing pSBAE coating. The results showed that the pristine glass and the PG-coated region do not have any sulfur (Figure 4). No

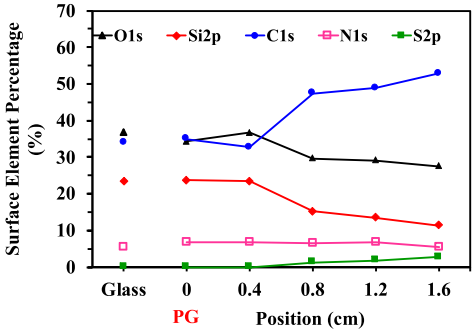

Figure 4. Elemental compositions on several locations of the pSBAE gradient surface. The gradient was created on a glass slide from a solution of PG (6 mg/mL), pSBAE (40 mg/mL), and APS (9 mg/mL). XPS analysis was performed at several locations over the gradient glass slide: glass, 0 (PG), 0.4, 0.8, 1.2, and 1.6 cm.

sulfur signal was detected in the 0.4 cm region, although the measurement of the WCA indicates an increase in hydrophilicity compared to PG. Sulfur was found at the 0.8, 1.2, and 1.6 cm spots with a value of 1.23, 1.745, and 2.66%, respectively (Figure 4). The XPS measurement also confirms the formation of a PG/pSBAE gradient coating over the glass slide.

The surface roughness at the different locations (Glass, 0 (PG), 0.4, 0.8, 1.2, and 1.6 cm) was determined using AFM, as

https://doi.org/10.1021/acsomega.1c06798
ACS Omega 2022, 7, 7125−7133

shown in Figure 5. The surface roughness of the PG substrate was 0.46 ± 0.04 nm, which is similar to that of the glass (0.40 ± 0.03 nm), indicating a smooth and uniform deposition of PG on the glass surface. The deposition of pSBAE increased the surface roughness with increasing deposition time. We found that the deposition of pSBAE generated linear protuberances. The roughness was increased to a plateau value of ~2.27 nm at 1.6 cm. Although the PG/pSBAE coating increased the surface roughness, the difference was very small, which might not affect cell adhesion significantly.

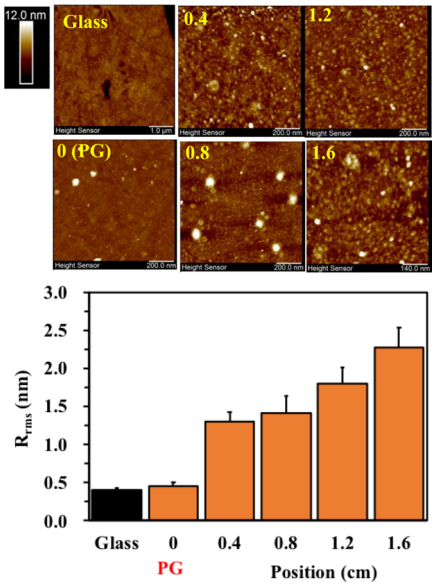

Figure 5. Gradient was created on a glass slide from a solution of PG (6 mg/mL), pSBAE (40 mg/mL), and APS (9 mg/mL). The surface roughness was determined using AFM at the different locations: glass, 0 (PG), 0.4, 0.8, 1.2, and 1.6 cm. n = 3.

2.4. Cell Adhesion and Protein Adsorption to Gradient Surfaces. The adhesion of L929 and MG63 cells was investigated on the gradient surface. L929 cells adhered and spread well on PG, while the number of cells decreased and the morphology of cells became round (Figure 6A). The cell number and the cellular spreading area decreased along the pSBAE gradient. We found that compared to the number of cells on PG, the adhesion of the cells was reduced to 69.2, 51.5, 32.1, and 19.8% at 0.4, 0.8, 1.2, and 1.6 cm, respectively (Figure 6B), indicating that a cell gradient was successfully created. The difference in cell numbers between 0 and 1.6 cm was ~5-folds. The cell spreading area also decreased from 634 μm^2 at 0 (PG) to 589, 561, 528, and 482 μm^2 at 0.4, 0.8, 1.2, and 1.6 cm, respectively (Figure 6C). The created pSBAE gradient generated a cell adhesion gradient with respect to the cell number and cell spreading.

The response of MG63 cells to the gradient surface was similar to that of L929 cells, that is, a decrease in both the number of cells and the spreading area along the gradient (Figure 7A). The decrease in the adhesion of MG63 cells was more abrupt along the gradient compared to that of L929 cells. The cell number at 0.4 cm was less than half of that of 0 (PG) (47.8%), and only 10.7% cell adhesion appeared at 1.6 cm (Figure 7B). The cell spreading area decreased greatly from 1093 μm^2 at 0 (PG) to 639 μm^2 at 0.4 cm (Figure 7C). The cell spreading area was reduced further to ~500 μm^2 from 0.8 to 1.6 cm.

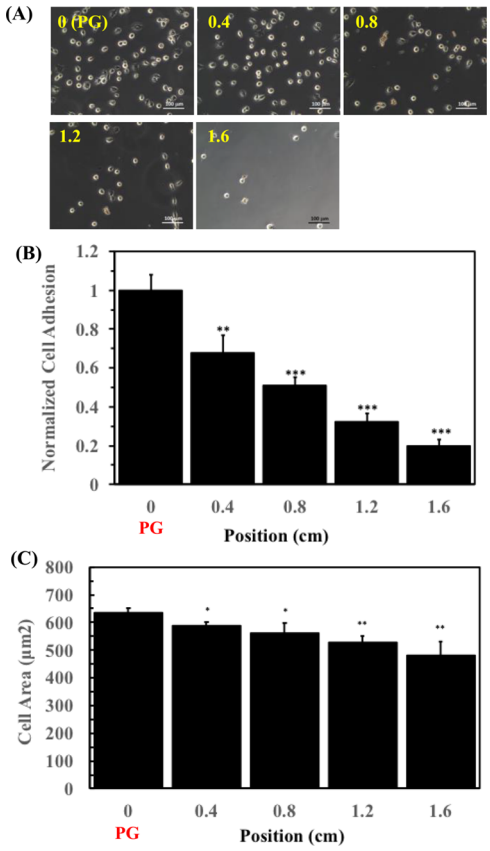

Figure 6. Adhesion of L929 cells on the gradient substrate. The gradient was created on a glass slide from a solution of PG (6 mg/mL), pSBAE (40 mg/mL), and APS (9 mg/mL). (A) Microscopic images of L929 cells at different locations. (B) Normalized cell adhesion to 0 (2.13×10^4 cells/cm^2) and (C) Averaged cell area of L929 cells. The values were determined randomly at five points at each location of a sample. The values from three samples were averaged. The error bars represent the standard deviation of three samples. *** $p < 0.001$, ** $p < 0.01$, and * $p < 0.05$ vs PG.

We successfully applied PG chemistry to fabricate a gradient substrate for cell adhesion. The gradients created using different APS ratios (3, 6, and 12 mg/mL) have shown a similar trend in mediating cell adhesion. The results are shown in the Supplementary Materials (Figures S8~S13).

Next, protein adsorption to the gradient surface was investigated. FITC-labeled BSA was used as a model protein. Protein adsorption at different locations was determined according to surface fluorescence and normalized to the fluorescence intensity at PG. The fluorescence intensity decreased linearly from PG to the pSBAE area (Figure 8). The fluorescence at 1.6 cm was about 40% of that at PG. The result shows that the pSBAE gradient surface resulted in a gradient of protein adsorption.

For poly(sulfobetaine), a zwitterionic polymer, when conjugated to a substrate, provides the antifouling capacity of the surface, by improving its wettability to attract water molecules to form a barrier to prevent nonspecific protein adsorption and cell adhesion.[44,49,59−61] The surface coverage of poly(sulfobetaine) affects the resistance of the substrate to cell adhesion and protein adsorption.[62] In this study, we showed that a gradient of pSBAE could be formed using the draining method.

https://doi.org/10.1021/acsomega.1c06798
ACS Omega 2022, 7, 7125−7133

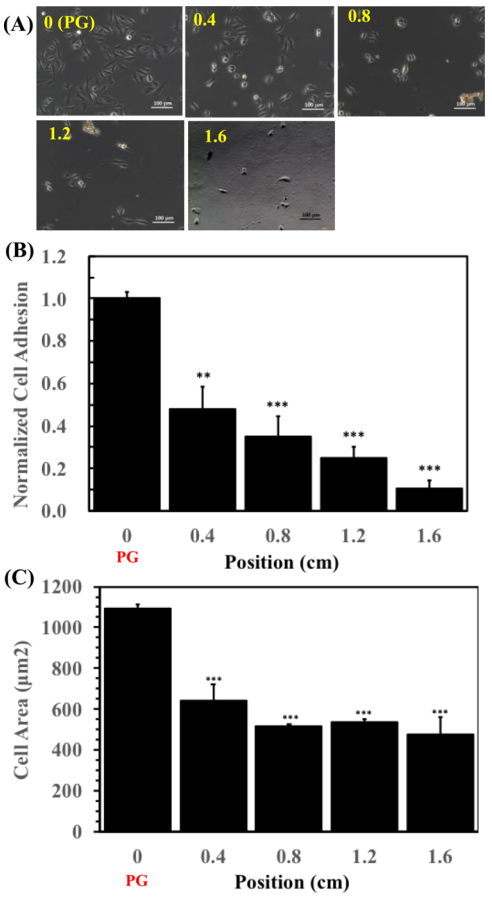

Figure 7. Adhesion of MG63 cells on the gradient substrate. (A) Microscopic images of MG-63 cells at different locations. (B) Normalized cell adhesion to that on 0 (2.62×10^4 cells/cm^2) and (C) Averaged cell area of MG63 cells for the condition APS = 9 mg/mL. The values were determined randomly at five points at each location of a sample. The values from three samples were averaged. The error bars represent the standard deviation of three samples. *** $p < 0.001$ and ** $p < 0.01$ vs. PG.

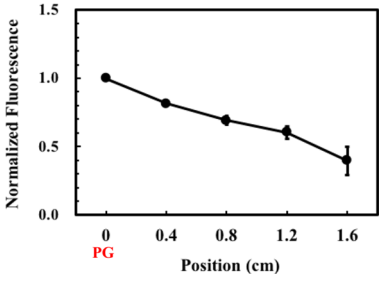

Figure 8. Protein adsorption on different regions of the gradient coating for APS = 9 mg/mL. The values were determined randomly at five points at each location of a sample. The values from three samples were averaged and normalized to the value of PG (0 cm).

The hydrophilicity of the glass slides increased with increasing incubation time in PG/pSBAE solution. The pSBAE gradient substrate results in gradients of cell adhesion and protein adsorption. Surface hydrophilicity increases with an increasing amount of bound pSBAE. To consider the relationship between surface wettability and biological interactions, we correlated surface wettability with cell adhesion and protein adsorption. The adhesion for both L929 cells and MG63 cells was correlated linearly with the WCAs (Figure 9). Similarly, BSA adsorption also showed a nice positive correlation with the WCAs in a polynomial

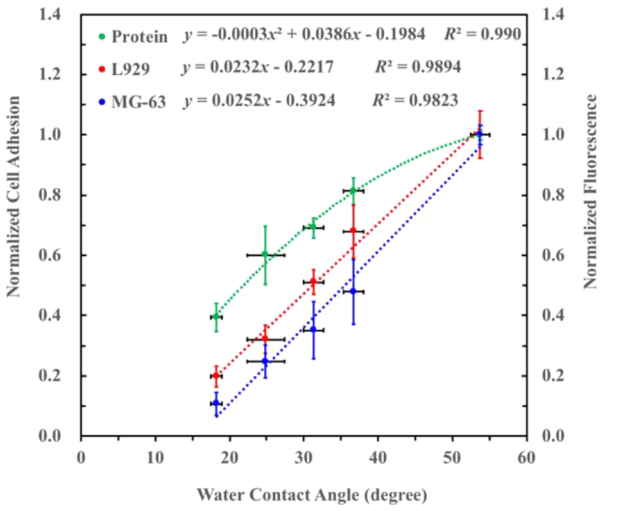

Figure 9. Correlation between the WCA and cell adhesion/protein adsorption.

pattern (Figure 9). Our results indicated that a pSBAE gradient was successfully fabricated using the draining method for the modulation of biointerfaces.

3. CONCLUSIONS

In this work, we developed a simple, fast, and economical method to develop continuous pSBAE gradient substrates. Oxidative polymerization of PG facilitates immobilization of antifouling pSBAE. The pSBAE gradient was prepared using the draining method in 7 min. Cell adhesion and protein adsorption were well correlated with surface wettability. We expect that this simple and faster method for the fabrication of a continuous chemical gradient is applicable for high-throughput screening of surface properties to modulate biointerfaces.

4. MATERIALS AND METHODS

4.1. Materials. Sulfobetaine methacrylate (SBMA, cat#537284) was purchased from Taiwan Hopax Chems (Kaohsiung, Taiwan). The following chemicals were purchased from Sigma-Aldrich, USA: 2-aminoethyl methacrylate hydrochloride (AEMA, cat.# 516155), azobisisobutyronitrile (AIBN, cat.# 78-67-1), ammonium persulfate (APS, cat.# A3678), pyrogallol (PG, cat.# P0381), albumin−fluorescein isothiocyanate conjugate (FITC-BSA, cat.# A9771), antibiotic-antimycotic solution (cat.# T4174), dimethyl sulfoxide (DMSO, cat.# 276855), 2-mercaptoethanol (cat.# M6250), and trypsin−ethylenediaminetetraacetic acid (EDTA) (cat.# T4174). Minimum essential medium alpha medium (α-MEM, cat.# 12000-022) and Dulbecco's modified Eagle medium−high glucose powder (DMEM−HG, cat.# 12100046) were purchased from GIBCO. Fetal bovine serum (FBS, cat.# 12003-500 M) was purchased from JRH Biosciences (Australia).

4.2. Synthesis and Characterization of pSBAE. A copolymer of SBMA and AEMA was synthesized using the ATRP polymerization method, as previously described.[44] Briefly, 0.848 g of SBMA and 0.049 g of AEMA were dissolved in 18 mL of deionized water. AIBN (5 mg) was dissolved in 2

https://doi.org/10.1021/acsomega.1c06798
ACS Omega 2022, 7, 7125−7133

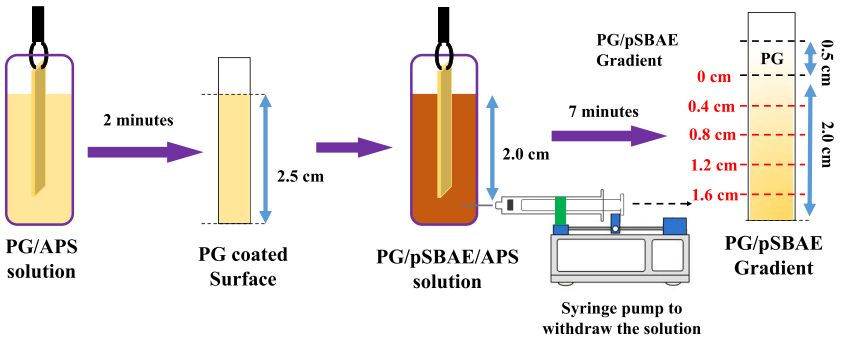

Figure 10. Schematic diagram of the gradient coating of PG/pSBAE. The red dashed lines in the rightmost slide indicate the positions for surface analysis, cell adhesion, and protein adsorption.

mL of DMSO and then added to the monomer solution dropwise with constant stirring. After the monomer solution was purged with nitrogen gas, its temperature was increased to 70 °C in an oil bath for 20 h. After the reaction, the product was dialyzed against deionized water and then freeze-dried. Gel permeation chromatography (Jasco, UV-2075, Japan) and nuclear magnetic resonance spectroscopy (NMR, Bruker AVIII HD 400 NMR, Germany) were used to determine the molecular weight and the chemical structure of the copolymer, respectively.

4.3. Gradient Coating of PG/pSBAE. Glass slides were cut into rectangular slides (0.7 cm × 3.0 cm) and then cleaned with methanol and deionized water under sonication. The glass slides were first immersed in the PG/APS solution (2 and 1 mg/mL in PBS, respectively) for 2 min to form a thin layer of PG on the glass substrates (Figure 10). After being rinsed with water, the PG-coated glass slides were placed vertically in a plastic tube containing a PG/pSBAE/APS solution. PG and pSBAE concentrations were fixed at 6 and 40 mg/mL, while the APS concentration was varied at 3, 6, 9, and 12 mg/mL. Glass slides were immersed at a length of 2 cm in the solution. The solution was withdrawn from a hole at the bottom of the tube using a syringe pump at a constant rate in 7 min. The slides were rinsed with water and then air-dried.

4.4. Surface Characterization. The PG/pSBAE gradient was analyzed using XPS, AFM, and static WCA measurement. The gradient area was divided by 4 lines, which were separated by 0.4 cm (red lines in the rightmost slide in Figure 10). The surface properties of the modified glass slides were characterized in pristine glass and along the 0 cm, 0.4, 0.8, 1.2, and 1.6 cm lines away from the border of the PG area. Because the 0 cm line was not very clear-cut, its surface characterization was done on the PG area. XPS and AFM were used to determine surface chemical elements and surface roughness, according to previous procedures.[44] The WCA was used to determine surface hydrophilicity.[44]

4.5. Cell Adhesion on PG/pSBAE Gradient Substrates. The modified glass slides were sterilized by UV exposure for 2 h, followed by immersion in 75% ethanol for 30 min. L929 cells or MG63 cells suspended in the culture medium were seeded on substrates at 2×10^4 cells/cm^2 and cultured for 24 h in a 37 °C incubator. The culture medium for L929 cells contained DMEM−HG, supplemented with 10% FBS, 10 mL of fungizone, 5 mL of gentamycin, and 0.4 mL of 2-mercaptoethanol in 1 L, pH 7.4. The culture medium for MG63 cells contained α-MEM medium supplemented with 10% FBS, 10 mL of fungizone, 5 mL of gentamycin, and 0.4 mL of 2-mercaptoethanol in 1 L. Unattached cells were rinsed with PBS. The attached cells were imaged at five different spots in every gradient area using a phase contrast microscope. Cell adhesion was determined by counting the number of cells in microscopic images, while the cell area was determined using the NIH ImageJ software. The values of cell adhesion were averaged in three gradient samples.

4.6. Adsorption of BSA. BSA adsorption to the gradient surface was evaluated using total internal reflection fluorescence.[44,63] Briefly, the gradient substrates were immersed in FITC-BSA solution (1 mg/mL in PBS) for 4 h at 37 °C, followed by rinsing with PBS to remove loosely bound FITC-BSA. Four fluorescent images were randomly taken at each location of the gradient surfaces using a fluorescent microscopy (Leica DM6000B Upright/OLYMPUS IX71 Inverted Microscope System, Germany) instrument. The total fluorescence of each image was quantified using NIH ImageJ and converted into the amount of adsorbed FITC-BSA. The fluorescence intensity at the PG/pSBAE gradient was normalized to that at PG. The values were averaged from three samples.

4.7. Statistical Analysis. Data were reported as mean ± standard deviation. Student's *t*-test was used to statistically analyze the data between different groups of the same sample. The probability of $p \leq 0.05$ was considered as a significant value. All statistical analyses were performed using the GraphPad Instat 3.0 program (GraphPad Software, La Jolla, CA).

■ ASSOCIATED CONTENT

Supporting Information

The Supporting Information is available free of charge at https://pubs.acs.org/doi/10.1021/acsomega.1c06798.

Figure S1: ^{1}H NMR of pSBAE. Figure S2: Polymerization of PG in the presence of potassium iodate. Figure S3: Polymerization of PG in the presence of sodium periodate. Figure S4: Polymerization of PG in the presence of copper sulfate. Figure S5: Polymerization of PG in the presence of potassium chlorate. Figure S6: Polymerization of PG in the presence of 20% methanol. Figure S7: Polymerization of PG in the presence of sodium persulfate. Figure S8: Adhesion of L929 cells on the gradient substrate for APS = 3 mg/mL. Figure S9: Adhesion of L929 cells on the gradient substrate for APS = 6 mg/mL. Figure S10: Adhesion of L929 cells on the gradient substrate for APS = 12 mg/mL. Figure S11: Adhesion of MG63 cells on the gradient substrate for APS = 3 mg/mL. Figure S12: Adhesion of MG63 cells on the gradient substrate for APS = 6 mg/mL. Figure

https://doi.org/10.1021/acsomega.1c06798
ACS Omega 2022, 7, 7125−7133

S13: Adhesion of MG63 cells on the gradient substrate for APS = 12 mg/mL (PDF)

AUTHOR INFORMATION

Corresponding Author

Wei-Bor Tsai − *Department of Chemical Engineering, National Taiwan University, Taipei 10617, Taiwan;* orcid.org/0000-0002-2316-5751; Email: weibortsai@ntu.edu.tw

Authors

Piyush Deval − *Department of Chemical Engineering, National Taiwan University, Taipei 10617, Taiwan;* orcid.org/0000-0003-4766-6195

Chia-Hsuan Lin − *Department of Material Science and Engineering, National Taiwan University, Taipei 10617, Taiwan*

Complete contact information is available at: https://pubs.acs.org/10.1021/acsomega.1c06798

Author Contributions

P.D.: investigation, formal analysis, design of methodology, and writing—original draft. C.-H.L.: AFM experiment and analysis. W.-B.T.: conceptualization, design of methodology, supervision, funding acquisition, and writing—review and editing.

Funding

The Ministry of Science and Technology of Taiwan (107-2221-E-002-109-MY3).

Notes

The authors declare no competing financial interest.

ACKNOWLEDGMENTS

We thank Professor Shyh-Chyang Luo at the Department of Materials Science and Engineering, National Taiwan University, for providing AFM.

ABBREVIATIONS

AEMA, 2-aminoethyl methacrylate; AFM, atomic force microscopy; AIBN, azobisisobutyronitrile; APS, ammonium persulfate; BSA, bovine serum albumin; DMEM−HG, Dulbecco's modified Eagle medium−high glucose; DMSO, dimethyl sulfoxide; DOPA, dopamine; FITC-BSA, albumin−fluorescein isothiocyanate conjugate; PEG, poly(ethylene glycol); α-MEM, minimum essential medium alpha medium; NMR, nuclear magnetic resonance spectroscopy; PG, pyrogallol; pSBAE, poly(sulfobetaine methac-rylate-*co*-2-aminoethyl methacrylate); SBMA, sulfobetaine methacrylate; WCA, water contact angle; XPS, X-ray photoelectron spectroscopy

REFERENCES

(1) Khang, G. Evolution of gradient concept for the application of regenerative medicine. *Biosurf. Biotrigology* **2015**, *1*, 202−213.

(2) Yang, L. L.; Pijuan-Galito, S.; Rho, H. S.; Vasilevich, A. S.; Eren, A. D.; Ge, L.; Habibovic, P.; Alexander, M. R.; de Boer, J.; Carlier, A.; van Rijn, P.; Zhou, Q. H. High-Throughput Methods in the Discovery and Study of Biomaterials and Materiobiology. *Chem. Rev.* **2021**, *121*, 4561−4677.

(3) Marklein, R. A.; Burdick, J. A. Spatially controlled hydrogel mechanics to modulate stem cell interactions. *Soft Matter* **2010**, *6*, 136−143.

(4) Faia-Torres, A. B.; Guimond-Lischer, S.; Rottmar, M.; Charnley, M.; Goren, T.; Maniura-Weber, K.; Spencer, N. D.; Reis, R. L.; Textor, M.; Neves, N. M. Differential regulation of osteogenic differentiation of stem cells on surface roughness gradients. *Biomaterials* **2014**, *35*, 9023−9032.

(5) Kunzler, T. P.; Drobek, T.; Sprecher, C. M.; Schuler, M.; Spencer, N. D. Fabrication of material-independent morphology gradients for high-throughput applications. *Appl. Surf. Sci.* **2006**, *253*, 2148−2153.

(6) Wang, P. Y.; Clements, L. R.; Thissen, H.; Jane, A.; Tsai, W. B.; Voelcker, N. H. Screening mesenchymal stem cell attachment and differentiation on porous silicon gradients. *Adv. Funct. Mater.* **2012**, *22*, 3414−3423.

(7) Oh, S. H.; Kim, T. H.; Im, G. I.; Lee, J. H. Investigation of pore size effect on chondrogenic differentiation of adipose stem cells using a pore size gradient scaffold. *Biomacromolecules* **2010**, *11*, 1948−1955.

(8) Wang, P. Y.; Tsai, W. B.; Voelcker, N. H. Screening of rat mesenchymal stem cell behaviour on polydimethylsiloxane stiffness gradients. *Acta Biomater.* **2012**, *8*, 519−530.

(9) Morgenthaler, S.; Lee, S.; Zürcher, S.; Spencer, N. D. A simple, reproducible approach to the preparation of surface-chemical gradients. *Langmuir* **2003**, *19*, 10459−10462.

(10) Julthongpiput, D.; Fasolka, M. J.; Zhang, W. H.; Nguyen, T.; Amis, E. J. Gradient chemical micropatterns: A reference substrate for surface nanometrology. *Nano Lett.* **2005**, *5*, 1535−1540.

(11) Zaari, N.; Rajagopalan, P.; Kim, S. K.; Engler, A. J.; Wong, J. Y. Photopolymerization in microfluidic gradient generators: Microscale control of substrate compliance to manipulate cell response. *Adv. Mater.* **2004**, *16*, 2133.

(12) Wang, P.-Y.; Clements, L. R.; Thissen, H.; Tsai, W.-B.; Voelcker, N. H. High-throughput characterisation of osteogenic differentiation of human mesenchymal stem cells using pore size gradients on porous alumina. *Biomater. Sci.* **2013**, *1*, 924−932.

(13) Cantini, M.; Sousa, M.; Moratal, D.; Mano, J. F.; Salmerón-Sánchez, M. Non-monotonic cell differentiation pattern on extreme wettability gradients. *Biomater. Sci.* **2013**, *1*, 202−212.

(14) Wang, P.-Y.; Clements, L. R.; Thissen, H.; Tsai, W.-B.; Voelcker, N. H. Screening rat mesenchymal stem cell attachment and differentiation on surface chemistries using plasma polymer gradients. *Acta Biomater.* **2015**, *11*, 58−67.

(15) Iwasaki, Y.; Sawada, S.-I.; Nakabayashi, N.; Khang, G.; Lee, H. B.; Ishihara, K. The effect of the chemical structure of the phospholipid polymer on fibronectin adsorption and fibroblast adhesion on the gradient phospholipid surface. *Biomaterials* **1999**, *20*, 2185−2191.

(16) Kim, M. S.; Seo, K. S.; Khang, G.; Lee, H. B. Preparation of a gradient biotinylated polyethylene surface to bind streptavidin−FITC. *Bioconjugate Chem.* **2005**, *16*, 245−249.

(17) Blondiaux, N.; Zurcher, S.; Liley, M.; Spencer, N. D. Fabrication of multiscale surface-chemical gradients by means of photocatalytic lithography. *Langmuir* **2007**, *23*, 3489−3494.

(18) Ding, Y. X.; Streitmatter, S.; Wright, B. E.; Hlady, V. Spatial Variation of the Charge and Sulfur Oxidation State in a Surface Gradient Affects Plasma Protein Adsorption. *Langmuir* **2010**, *26*, 12140−12146.

(19) Tan, H. P.; Wan, L.; Wu, J. D.; Gao, C. Y. Microscale control over collagen gradient on poly(L-lactide) membrane surface for manipulating chondrocyte distribution. *Colloids Surf., B* **2008**, *67*, 210−215.

(20) Mougin, K.; Ham, A. S.; Lawrence, M. B.; Fernandez, E. J.; Hillier, A. C. Construction of a tethered poly(ethylene glycol) surface gradient for studies of cell adhesion kinetics. *Langmuir* **2005**, *21*, 4809−4812.

(21) Zhang, Z.; Zhang, M.; Chen, S. F.; Horbetta, T. A.; Ratner, B. D.; Jiang, S. Y. Blood compatibility of surfaces with superlow protein adsorption. *Biomaterials* **2008**, *29*, 4285−4291.

(22) Chen, Y.; Luo, S. C. Synergistic Effects of Ions and Surface Potentials on Antifouling Poly(3,4-ethylenedioxythiophene): Com-

parison of Oligo(Ethylene Glycol) and Phosphorylcholine. *Langmuir* **2019**, *35*, 1199−1210.
(23) Chen, S. F.; Zheng, J.; Li, L. Y.; Jiang, S. Y. Strong resistance of phosphorylcholine self-assembled monolayers to protein adsorption: Insights into nonfouling properties of zwitterionic materials. *J. Am. Chem. Soc.* **2005**, *127*, 14473−14478.
(24) Yeon, D. K.; Ko, S.; Jeong, S.; Hong, S. P.; Kang, S. M.; Cho, W. K. Oxidation-Mediated, Zwitterionic Polydopamine Coatings for Marine Antifouling Applications. *Langmuir* **2019**, *35*, 1227−1234.
(25) Lin, X. J.; Jain, P.; Wu, K.; Hong, D.; Hung, H. C.; O'Kelly, M. B.; Li, B. W.; Zhang, P.; Yuan, Z. F.; Jiang, S. Y. Ultralow Fouling and Functionalizable Surface Chemistry Based on Zwitterionic Carboxybetaine Random Copolymers. *Langmuir* **2019**, *35*, 1544−1551.
(26) Huang, C. J.; Zheng, Y. Y. Controlled Silanization Using Functional Silatrane for Thin and Homogeneous Antifouling Coatings. *Langmuir* **2019**, *35*, 1662−1671.
(27) Venault, A.; Chang, Y. Designs of Zwitterionic Interfaces and Membranes. *Langmuir* **2019**, *35*, 1714−1726.
(28) He, Y.; Hower, J.; Chen, S. F.; Bernards, M. T.; Chang, Y.; Jiang, S. Y. Molecular simulation studies of protein interactions with zwitterionic phosphorylcholine self-assembled monolayers in the presence of water. *Langmuir* **2008**, *24*, 10358−10364.
(29) Han, X. F.; Leng, C.; Shao, Q.; Jiang, S. Y.; Chen, Z. Absolute Orientations of Water Molecules at Zwitterionic Polymer Interfaces and Interfacial Dynamics after Salt Exposure. *Langmuir* **2019**, *35*, 1327−1334.
(30) Zhang, Z.; Chao, T.; Chen, S. F.; Jiang, S. Y. Superlow fouling sulfobetaine and carboxybetaine polymers on glass slides. *Langmuir* **2006**, *22*, 10072−10077.
(31) Cheng, F.; Zhu, C. L.; He, W.; Zhao, J.; Qu, J. P. pSBMA-Conjugated Magnetic Nanoparticles for Selective IgG Separation. *Langmuir* **2019**, *35*, 1111−1118.
(32) Ulusan, S.; Butun, V.; Banerjee, S.; Erel-Goktepe, I. Biologically Functional Ultrathin Films Made of Zwitterionic Block Copolymer Micelles. *Langmuir* **2019**, *35*, 1156−1171.
(33) Qin, Z. H.; Chen, T. T.; Teng, W. Z.; Jin, Q.; Ji, J. Mixed-Charged Zwitterionic Polymeric Micelles for Tumor Acidic Environment Responsive Intracellular Drug Delivery. *Langmuir* **2019**, *35*, 1242−1248.
(34) Lin, W. F.; Ma, G. L.; Yuan, Z. F.; Qian, H. F.; Xu, L. B.; Sidransky, E.; Chen, S. F. Development of Zwitterionic Polypeptide Nanoformulation with High Doxorubicin Loading Content for Targeted Drug Delivery. *Langmuir* **2019**, *35*, 1273−1283.
(35) Chen, S. H.; Fukazawa, K.; Inoue, Y.; Ishihara, K. Photoinduced Surface Zwitterionization for Antifouling of Porous Polymer Substrates. *Langmuir* **2019**, *35*, 1312−1319.
(36) De Vera, J. S.; Venault, A.; Chou, Y. N.; Tayo, L.; Chiang, H. C.; Aimar, P.; Chang, Y. Self-Cleaning Interfaces of Polydimethylsiloxane Grafted with pH-Responsive Zwitterionic Copolymers. *Langmuir* **2019**, *35*, 1357−1368.
(37) Li, W. C.; Chu, K. W.; Liu, L. Y. Zwitterionic Gel Coating Endows Gold Nanoparticles with Ultrastability. *Langmuir* **2019**, *35*, 1369−1378.
(38) Zhang, J.; Chen, L. Q.; Chen, J. D.; Zhang, Q.; Feng, J. Stability, Cellular Uptake, and in Vivo Tracking of Zwitterion Modified Graphene Oxide as a Drug Carrier. *Langmuir* **2019**, *35*, 1495−1502.
(39) Song, J. Y.; Zhu, Y. N.; Zhang, J. M.; Yang, J.; Du, Y.; Zheng, W. W.; Wen, C. Y.; Zhang, Y. M.; Zhang, L. Encapsulation of AgNPs within Zwitterionic Hydrogels for Highly Efficient and Antifouling Catalysis in Biological Environments. *Langmuir* **2019**, *35*, 1563−1570.
(40) Wang, Y. S.; Yau, S.; Chau, L. K.; Mohamed, A.; Huang, C. J. Functional Biointerfaces Based on Mixed Zwitterionic Self-Assembled Monolayers for Biosensing Applications. *Langmuir* **2019**, *35*, 1652−1661.
(41) Ishihara, K. Blood-Compatible Surfaces with Phosphorylcholine-Based Polymers for Cardiovascular Medical Devices. *Langmuir* **2019**, *35*, 1778−1787.
(42) Pei, J.; Hall, H.; Spencer, N. D. The role of plasma proteins in cell adhesion to PEG surface-density-gradient-modified titanium oxide. *Biomaterials* **2011**, *32*, 8968−8978.
(43) Ren, T.; Yu, S.; Mao, Z.; Gao, C. A complementary density gradient of zwitterionic polymer brushes and NCAM peptides for selectively controlling directional migration of Schwann cells. *Biomaterials* **2015**, *56*, 58−67.
(44) Yeh, S.-L.; Wang, T.-C.; Yusa, S.-I.; Thissen, H.; Tsai, W.-B. Conjugation of Polysulfobetaine via Poly(pyrogallol) Coatings for Improving the Antifouling Efficacy of Biomaterials. *ACS Omega* **2021**, *6*, 3517−3524.
(45) Sileika, T. S.; Barrett, D. G.; Zhang, R.; Lau, K. H. A.; Messersmith, P. B. Colorless multifunctional coatings inspired by polyphenols found in tea, chocolate, and wine. *Angew. Chem., Int. Ed.* **2013**, *52*, 10766−10770.
(46) Lee, H.; Dellatore, S. M.; Miller, W. M.; Messersmith, P. B. Mussel-inspired surface chemistry for multifunctional coatings. *Science* **2007**, *318*, 426−430.
(47) Thissen, H.; Koegler, A.; Salwiczek, M.; Easton, C. D.; Qu, Y.; Lithgow, T.; Evans, R. A. Prebiotic-chemistry inspired polymer coatings for biomedical and material science applications. *NPG Asia Mater.* **2015**, *7*, e225.
(48) Sileika, T. S.; Barrett, D. G.; Zhang, R.; Lau, K. H. A.; Messersmith, P. B. Colorless multifunctional coatings inspired by polyphenols found in tea, chocolate, and wine. *Am. Ethnol.* **2013**, *125*, 10966−10970.
(49) Chen, W.-H.; Liao, T.-Y.; Thissen, H.; Tsai, W.-B. One-step aminomalononitrile-based coatings containing zwitterionic copolymers for the reduction of biofouling and the foreign body response. *ACS Biomater. Sci. Eng.* **2019**, *5*, 6454−6462.
(50) Liao, T.-Y.; Easton, C. D.; Thissen, H.; Tsai, W.-B. Aminomalononitrile-assisted multifunctional antibacterial coatings. *ACS Biomater. Sci. Eng.* **2020**, *6*, 3349−3360.
(51) Tsai, W.-B.; Chien, C.-Y.; Thissen, H.; Lai, J.-Y. Dopamine-assisted immobilization of poly(ethylene imine) based polymers for control of cell−surface interactions. *Acta Biomater.* **2011**, *7*, 2518−2525.
(52) Wu, M. B.; Fan, X. L.; Yang, H. C.; Yang, J.; Zhu, M. M.; Ren, K. F.; Ji, J.; Xu, Z. K. Ultrafast formation of pyrogallol/polyethyleneimine nanofilms for aqueous and organic nanofiltration. *J. Membrane Sci.* **2019**, *570*, 270−277.
(53) Wang, Y.; Park, J. P.; Hong, S. H.; Lee, H. Biologically Inspired Materials Exhibiting Repeatable Regeneration with Self-Sealing Capabilities without External Stimuli or Catalysts. *Adv. Mater.* **2016**, *28*, 9961−9968.
(54) Chang, C.-C.; Letteri, R.; Hayward, R. C.; Emrick, T. Functional sulfobetaine polymers: synthesis and salt-responsive stabilization of oil-in-water droplets. *Macromol.* **2015**, *48*, 7843−7850.
(55) Wei, Q.; Zhang, F.; Li, J.; Li, B.; Zhao, C. Oxidant-induced dopamine polymerization for multifunctional coatings. *Polym. Chem.* **2010**, *1*, 1430−1433.
(56) Yue, Q.; Wang, M.; Sun, Z.; Wang, C.; Wang, C.; Deng, Y.; Zhao, D. A versatile ethanol-mediated polymerization of dopamine for efficient surface modification and the construction of functional core−shell nanostructures. *J. Mater. Chem. B* **2013**, *1*, 6085−6093.
(57) Hong, S. H.; Hong, S.; Ryou, M. H.; Choi, J. W.; Kang, S. M.; Lee, H. Sprayable ultrafast polydopamine surface modifications. *Adv. Mater. Interfaces* **2016**, *3*, No. 1500857.
(58) Zhang, C.; Ou, Y.; Lei, W. X.; Wan, L. S.; Ji, J.; Xu, Z. K. $CuSO_4/H_2O_2$-induced rapid deposition of polydopamine coatings with high uniformity and enhanced stability. *Angew. Chem., Int. Ed.* **2016**, *55*, 3054−3057.
(59) Chang, Y.; Chang, W.-J.; Shih, Y.-J.; Wei, T.-C.; Hsiue, G.-H. Zwitterionic sulfobetaine-grafted poly (vinylidene fluoride) membrane with highly effective blood compatibility via atmospheric plasma-induced surface copolymerization. *ACS Appl. Mater. Interfaces* **2011**, *3*, 1228−1237.
(60) Chen, L.; Tan, L.; Liu, S.; Bai, L.; Wang, Y. Surface modification by grafting of poly (SBMA-co-AEMA)-g-PDA coating

https://doi.org/10.1021/acsomega.1c06798
ACS Omega 2022, 7, 7125−7133

and its application in CE. *J. Biomater. Sci., Polym. Ed.* **2014**, *25*, 766−785.
(61) Kuo, W.-H.; Wang, M.-J.; Chien, H.-W.; Wei, T.-C.; Lee, C.; Tsai, W.-B. Surface modification with poly(sulfobetaine methacrylate-co-acrylic acid) to reduce fibrinogen adsorption, platelet adhesion, and plasma coagulation. *Biomacromolecules* **2011**, *12*, 4348−4356.
(62) Chou, Y.-N.; Wen, T.-C.; Chang, Y. Zwitterionic surface grafting of epoxylated sulfobetaine copolymers for the development of stealth biomaterial interfaces. *Acta Biomater.* **2016**, *40*, 78−91.
(63) Lok, B. K.; Cheng, Y.-L.; Robertson, C. R. Protein adsorption on crosslinked polydimethylsiloxane using total internal reflection fluorescence. *J. Colloid Interface Sci.* **1983**, *91*, 104−116.

https://doi.org/10.1021/acsomega.1c06798
ACS Omega 2022, 7, 7125−7133